Improvement of Simplex Meshes Model for 3D Hippocampus Segmentation

M. M. Karimi [1] N. Batmanghelich [1,2] H. Soltanian-Zadeh [1,2,3] C. Lucas [1,2]

[1] University of Tehran [2] Institute for Studies in Theoretical Physics and Mathematic [3] Henry Ford Health System

Electrical engineering department, University of Tehran, Tehran, 14395/515

Iran

m.karimi@ece.ut.ac.ir, k.batman@ece.ut.ac.ir, hszadeh@ut.ac.ir, lucas@ipm.ir

ABSTRACT

In this paper, we used a deformable surface model, called simplex meshes, for hippocampus segmentation in brain MRI. Major problems of the hippocampus segmentation are weak edges and noise that may cause deformable model to move in wrong ways. To overcome these problems, we used simplex meshes model, which has the capability to move roughly. To initialize the primary shape we projected an atlas to the real data using a registration algorithm. We selected some parts of the initial shape and exerted forces to the vertices of this shape, which is proportion to the distance to these parts. Displacement of these parts helps model to overcome weak edges and also prevents self-cutting of the vertices. Finally, we did a final tuning to reach to the small details of the edges.

KEY WORDS

Simplex meshes, Deformable surface, brain segmentation, Magnetic Resonance Imaging (MRI)

1. Introduction

Simplex meshes model is a discrete model for the representation of a surface with arbitrary shape. This model has the capability to find a close shape or a shape with holes on its surface [1]. We use this model for hippocampus segmentation because computation of some features of surface such as curvature is easier in this model than other ones. Simplex meshes are capable to move to the surface of an object with multi level of rigidity [2]. This model uses internal and external forces like other discrete deformable surfaces to move to the edges of an object. Deformation of this model has two steps:

1. In the first few iterations, it moves rigidly and has rough movement.
2. After reaching to the vicinity of the borders, it moves with details.

We propose a method to improve the first step of this model deformation and also a method to overcome the self-cutting problem of the vertices of 3D models. We propose a surface like a balloon. When you push your finger to a balloon, all the points which are near your finger also will be pushed, but they will move less than where you put your finger. This movement prevents from arbitrary displacement of vertices, which may cause self-cutting.

We implemented this method for hippocampus segmentation, which has discontinuous edges. Noise and artifacts have made the segmentation of hippocampus challenging [3]. In addition to these problems, hippocampus does not have clear superior border with amygdala, especially on coronal views. Slice by slice segmentation of this structure does not generate desired results because all the landmarks of this structure are not seen on the 2D views [4]. Thus, we used a 3D model that can move to arbitrary direction rigidly or with details.

2. Related Work

Deformable surfaces are new generations of deformable models. The first generations are dynamic contours used for 2D segmentations [5], [6], [7]. But because deformable surfaces are able to use more information than dynamic contours to find an object in a volume, they are preferred. Two different kinds of deformable surfaces are now available: stochastic and non-stochastic models. Stochastic models are based on Cootes et. al. [8] efforts on active shapes and surface models. Non-stochastic models use rule-based methods that are based on information obtained from radiologists [9].

3. Original Model

Simplex meshes model includes some vertices and faces. In this model, each vertex is connected to only three vertices. Simplex meshes can be extracted from a triangulation algorithm such as iso-surface method. There is a duality between triangulation models and simplex meshes model [2] (Fig. 1. a).

As seen in Fig.1, each vertex is connected to only three neighbors. The position of vertex i is represented by $\mathbf{P}_i$. At each vertex, the normal direction is computed by:

$$\mathbf{n}_i = \frac{\mathbf{P}_{N_1(i)} \times \mathbf{P}_{N_2(i)} + \mathbf{P}_{N_2(i)} \times \mathbf{P}_{N_3(i)} + \mathbf{P}_{N_3(i)} \times \mathbf{P}_{N_1(i)}}{\left\| \mathbf{P}_{N_1(i)} \times \mathbf{P}_{N_2(i)} + \mathbf{P}_{N_2(i)} \times \mathbf{P}_{N_2(i)} + \mathbf{P}_{N_2(i)} \times \mathbf{P}_{N_3(i)} \right\|} \quad (1)$$

The simplex angle φ_i at each vertex is defined with the following two equations:

$$\sin(\varphi_i) = \frac{r_i}{R_i} sign(\mathbf{P}_i \mathbf{P}_{N_1(i)} . \mathbf{n}_i) \quad (2)$$

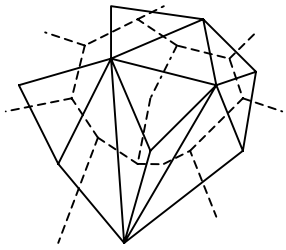

(a)

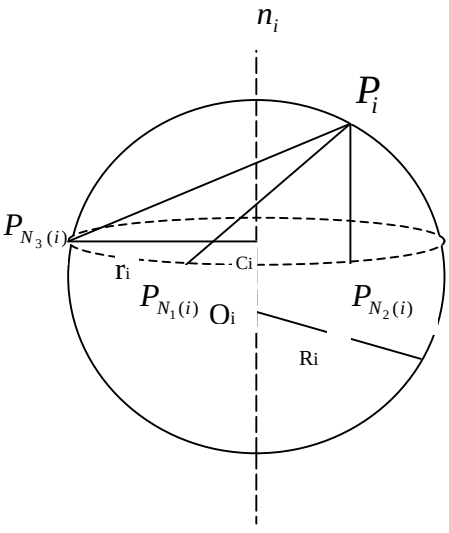

(b)

Fig. 1. (a) Duality between triangulation and simplex meshes. Solid lines are lines of triangulation. (b) A typical vertex with its three neighbors.

$$\cos(\varphi_i) = \frac{\left\| O_i C_i \right\|}{R_i} sign(O_i C_i . \mathbf{n}_i) \quad (3)$$

where S_2 is a sphere of center O_i and radius R_i constructed from four vertices $\mathbf{P}_i, \mathbf{P}_{N_1(i)}, \mathbf{P}_{N_2(i)}, \mathbf{P}_{N_3(i)}$ and S_1 is a circle of center C_i and radius r_i made from three vertices $\mathbf{P}_{N_1(i)}, \mathbf{P}_{N_2(i)}, \mathbf{P}_{N_3(i)}$.

We can model each vertex of simplex meshes with φ_i and three metric parameters $\varepsilon_i^1, \varepsilon_i^2, \varepsilon_i^3$:

$$\mathbf{P}_i = \varepsilon_i^1 \mathbf{P}_{N_1(i)} + \varepsilon_i^2 \mathbf{P}_{N_2(i)} + \varepsilon_i^3 \mathbf{P}_{N_3(i)} + L(r_i, d_i, \varphi_i) \mathbf{n}_i \quad (4)$$

$$L(r_i, d_i, \varphi_i) = \frac{(r_i^2 - d_i^2)\tan(\varphi_i)}{\varepsilon \sqrt{r_i^2 + (r_i^2 - d_i^2)\tan^2(\varphi_i) + r_i}}$$

where d_i is the distance between projection of $\mathbf{P}_i$ in the plane constructed by its three neighbors and C_i.

4. Initialization

- An atlas of hippocampus was constructed from MRI images of several subjects. Using FLIRT software [10] this reference volume was registered on each new volume. FLIRT applied an affine transform only. Then using the matrix obtained from FLIRT, atlas of hippocampus was projected to the new subject and initial shape was constructed.
- After initialization, iso-surface algorithm on the initial shape was executed and triangulation model of the surface was extracted.
- From duality property of simplex meshes with triangulation [1], vertices and faces of simplex meshes were extracted.

5. Deformation Process

5. 1 Rough Movement

Most of the deformable surfaces used for hippocampus segmentation without stochastic information use internal forces and external forces to deform to the target. Internal forces usually are defined to hold the model as smooth as possible. Internal forces are functions of curvatures of vertices and are exerted to pull the model to the minimum curvature at each vertex. On the contrary, external forces are exerted to pull the model to the boundary of the desired object. In 2D segmentation, intersection of vertices rarely happens if vertices move in the normal direction. But in the 3D volumes, self-cutting is a usual event when a model tries to deform.

To overcome this problem, all the vertices of a model were divided to *J* clusters. For each cluster, we found the center of the cluster (S_j) and the normal vector was

computed at the center of each cluster (n_j). For each vertex, a fuzzy membership function was introduced which determined the membership of each vertex to each cluster (u_{ij}). We used Euclidean distance for the definition of u_{ij}:

$$u_{ij} = \frac{1}{1 + d(\mathbf{P}_i, \mathbf{S}_j)} \quad (5)$$

Using this definition, we introduced new forces as:

$$\mathbf{F}_i = \sum_{j=1}^{J} u_{ij} (\mathbf{F}_{ex,j} \cdot \mathbf{n}_j) \mathbf{n}_j \quad (6)$$

where:

$$\mathbf{F}_{ex,j} = \nabla^2 (I(x_j, y_j, z_j) * G_\sigma) \quad (7)$$

$$\mathbf{P}_i^{t+1} = \mathbf{P}_i^t + \beta_i \cdot \mathbf{F}_i \quad (8)$$

where G_σ is a 3D Gaussian kernel that smoothes the images and prevents the model to stick to the weak edges and β_i is a constant that adjusts the displacement of the vertex. No internal forces are defined in the rough deformation because the curvature continuity constraint will be satisfied with this special kind of deformation. A vertex moves mostly in the direction of the normal vector of the part that this vertex has the highest membership to it. If a vertex does not have dominant membership to one cluster, it will move in the normal direction of two or more clusters. This is like a balloon when you push it from two adjacent points. The points that are between these two points move smoothly in spite of the different directional movements (Fig. 2). This kind of deformation also solves the self-cutting problem because it prevents the vertices from huge movements and limits them around the center of the cluster which they have largest membership to it.

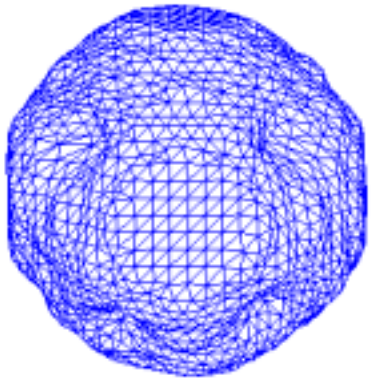

Fig. 2. Representation of the idea of rough movement on a sphere.

5.2 Final Tuning

After reaching to the vicinity of the shape border, the model will move to the border precisely and will find the details of the border. This step will be done like other deformable models. We used external forces defined in equation (7) and internal forces used in [2]:

$$\mathbf{F}_{\text{int}} = \mathbf{P}_i \mathbf{P}_i^* \quad (9)$$

where P_i^* is defined in equation (3). And ultimately:

$$\mathbf{F}_i = \alpha_i \mathbf{F}_{\text{int}} + \beta_i^* \mathbf{F}_{ex,i} \quad (10)$$

$$\mathbf{P}_i^{t+1} = \mathbf{P}_i^t + \lambda_i (\mathbf{P}_i^t - \mathbf{P}_i^{t-1}) + \mathbf{F}_i \quad (11)$$

λ_i is a damping factor. β_i^* is lower than β_i which is used in the rough deformation because after rough deformation, the model is in the vicinity of the border and does not require high external forces. Internal forces are defined based on the distance from current vertex position to the desired position. The desired constraints are exerted on P_i^* that attracts P_i to itself.

Different constraints that can exert on P_i^* are found in [1]. We used simplex angle constraint with rigidity factor of two. Ultimately the simplex meshes model was converted to the triangulation model for visualization.

6. Results

We implemented the proposed method on volume MRI images of 5 subjects whose manual expert segmentation of hippocampus were also available. This data was obtained from Internet Brain Segmentation Repository (IBSR). The total iterations that are required for the hippocampus segmentation is 100. Until iteration 30, the model deforms roughly and is fast but after this iteration because it wants to find details of the border takes long time to converge. We only found right hippocampus border for these patients. The inferior and anterior parts of the hippocampus were segmented precisely. The major problem was with superior parts. It is expected that the algorithm is not able to find the border between hippocampus and amygdala because there is no real edge between these structures in coronal views. But it could find this border well. The superior and medial part of hippocampus was the part that the model could not find the borders. The results of implementing this method on 5 subjects compared with manual expert segmentation are represented in Table 1. Different slices of the hippocampus segmentation are also shown in Fig. 3 to Fig. 5. We cut the surface for each slice representation.

7. Conclusion

In this paper, we applied and optimized simplex meshes model for the segmentation of hippocampus. We divided the segmentation process to two steps and also used an atlas for initialization. As seen in the results, the model could not find some parts of the hippocampus well. In the future work, we will try to move the model to the parts that are not segmented well currently.

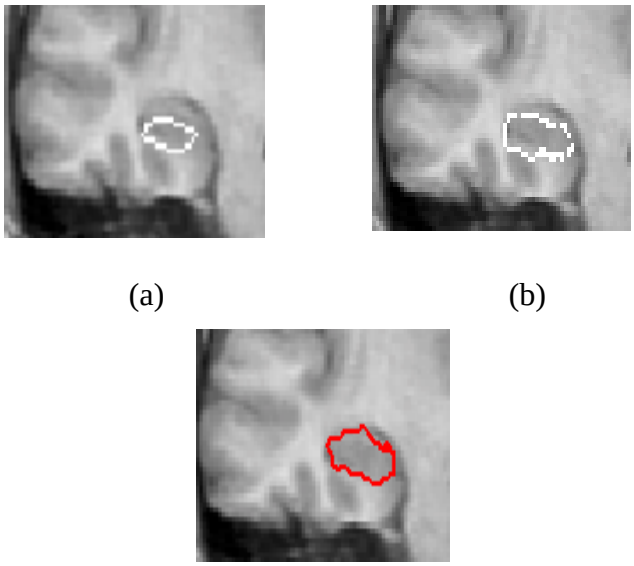

(a) (b)

(c)

Fig. 3. Deformation process on slice 59. (a) initial contour after registration (b) final cut of surface after deformation . (c) manual expert segmentation. It is seen that inferior part of hippocampus has been segmented very well.

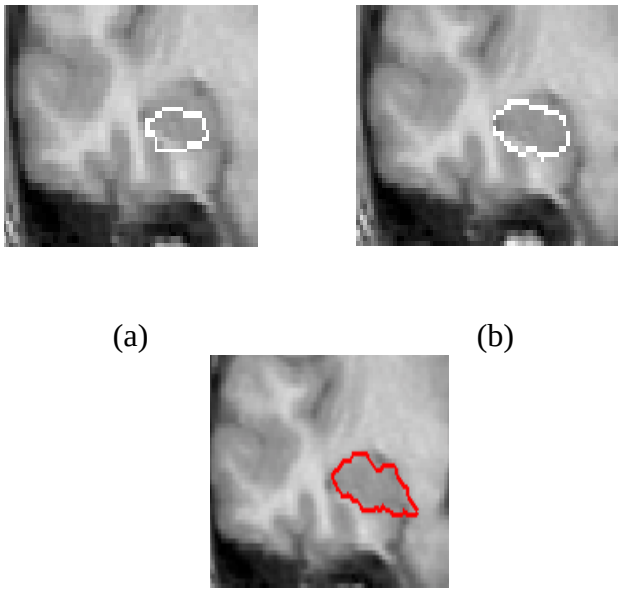

(a) (b)

(c)

Fig. 4. Deformation process on slice 61. (a) initial contour after registration (b) final cut of surface after deformation . (c) manual expert segmentation. At the superior and medial part of the hippocampus, the model could not find the borders.

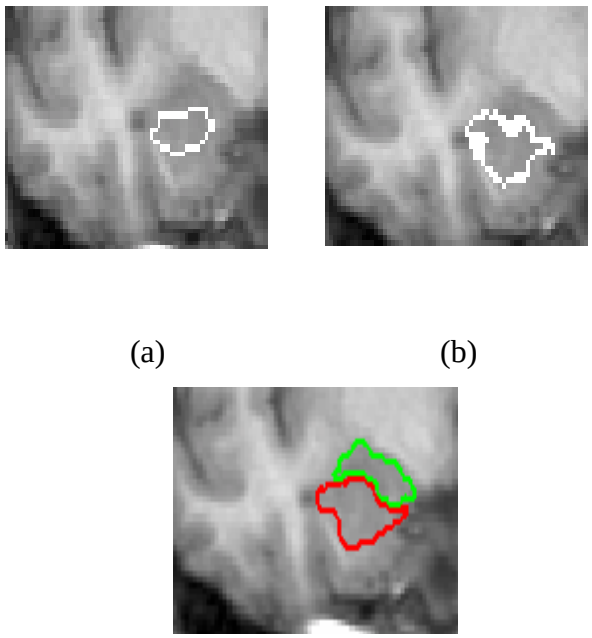

(a) (b)

(c)

Fig. 5. Deformation process on slice 61. This figure shows that the model does not penetrate to the amygdala body. The green structure in Figure (c) is amygdale. The reason for thickening of the border in figure (b) is the vertices put between two slices that are projected to the nearest slice when a surface is cut.

Table 1. Results of the implementation of the method on 5 different subjects for segmentation of body and head of the right hippocampus. The results show the percent of intersection between manual segmentation and initial shape and also between manual segmentation and segmentation obtained using the proposed method.

Subjects	1	2	3	4	5
Initial shape	62.4%	60.1%	63.2%	66.5%	59.4%
Final shape	85%	83.2%	87.3%	90.1%	81.8%

8. References

[1] H. Delingette, Simplex Meshes: a General Representation for3DShape Reconstruction, *Technical Report 2214, INRIA*, 1-75, 1994.

[2] H. Delingette, General object reconstruction based on simplex meshes, *International Jornal of Computer Vision 32*, 111-146, 1997.

[3]. A. Ghanei, and H. Soltanian-Zadeh, A Discrete Curvature-Based Deformable Surface Model with Application to segmentation of Volumetric Images, *IEEE Transactions on Information Ttechnology in Biomedicine*, 6(4), 285-295, DECEMBER 2002.

[4]. A. Convit, P. McHugh, O. T. Wolf, M. J. Deleon, M. Bobinski, S. De Santi, A. Roche, and W. Tsui, MRI volume of the amygdala: a reliable method allowing separation from the hippocampal formation , *Psychiatry Research: Neuroimaging Section (90)*, 113-123, 1999.

[5]. S. Lobregt, and M. A. Viergever, A Discrete Dynamiz Contour Model, *IEEE Transactions on Medical Imaging*, 14(1), 12-22, March 1995.

[6]. T. McInerney, and D. Terzepoulos, Deformable models in medical image analysis: a survey, *Medical Iamge analysis*, 1(2), 91-108, 1996.

[7] A. Ghanei, H. Soltanian-Zadeh, and J. P. Windham, Deformable model for hippocampus segmentation: Improvements and extension to 3-D, *in Proc. 1996 IEEE Nuclear Sci. Symp. Med. Image. Conf*, 1, 1797-1801, 1999.

[8]. T. F. Cootes, D. Cooper, C. J. Taylor, and J. Graham, Active Shape models-their training and application, *Computer vision and Image understanding*, 61(1), 38- 59, 1995.

[9] A. Pitiot, H. Delingette, N. Ayache, and P. M. Thompson, Expert Knowledge Guided Segmentation System for Brain MRI, *MICCAI (2)*, 644-652, 2003.

[10] M. Jenkinson, and S. Smith, A global optimization method for roboust affine registration of brain images, *Medical Iamge analysis*, 5(2), 143-156,